

## Molecular dispersion energy parameters for alkali and halide ions in aqueous solution

S. Reiser,<sup>1</sup> S. Deublein,<sup>1</sup> J. Vrabec,<sup>2</sup> and H. Hasse<sup>1, a)</sup>

<sup>1</sup>*Laboratory of Engineering Thermodynamics, University of Kaiserslautern,  
67663 Kaiserslautern, Germany*

<sup>2</sup>*Thermodynamics and Energy Technology, University of Paderborn,  
33098 Paderborn, Germany*

(Dated: 10 January 2014)

Thermodynamic properties of aqueous solutions containing alkali and halide ions are determined by molecular simulation. The following ions are studied: Li<sup>+</sup>, Na<sup>+</sup>, K<sup>+</sup>, Rb<sup>+</sup>, Cs<sup>+</sup>, F<sup>-</sup>, Cl<sup>-</sup>, Br<sup>-</sup> and I<sup>-</sup>. The employed ion force fields consist of one Lennard-Jones (LJ) site and one concentric point charge with a magnitude of  $\pm 1$  e. The SPC/E model is used for water. The LJ size parameter of the ion models is taken from Deublein et al. (J. Chem. Phys. **136**, 084501 (2012)), while the LJ energy parameter is determined in the present study based on experimental self-diffusion coefficient data of the alkali cations and the halide anions in aqueous solutions as well as the position of the first maximum of the radial distribution function of water around the ions. On the basis of these force field parameters, the electric conductivity, the hydration dynamics of water molecules around the ions and the enthalpy of hydration is predicted. Considering a wide range of salinity, this study is conducted at temperatures of 293.15 and 298.15 K and a pressure of 1 bar.

---

<sup>a)</sup>To whom correspondence should be addressed: hans.hasse@mv.uni-kl.de

## I. INTRODUCTION

Aqueous electrolyte solutions play an important role in many natural processes and technical applications. Their thermodynamic properties are dominated by the strong electrostatic interactions between the ions and the solvent molecules. However, not only charge and ionic strength are relevant, but also the individual nature of the ions. Most electrolyte solutions are outside of the regime which can be described with the approach by Debye and Hückel<sup>1,2</sup>. Therefore, different empirical extensions of the Debye-Hückel limiting law have been suggested<sup>3-7</sup>, which also consider the non-electrostatic interactions between the ions. These models introduce a large number of adjustable parameters so that they often serve as correlation tools only. Molecular simulations of electrolyte solutions go far beyond these models. They allow for detailed insights into the behavior of electrolyte solutions and for predictions of their properties. The prerequisite are, however, accurate molecular force fields.

For water, many force fields are available. The most common ones<sup>8</sup>, SPC<sup>9</sup>, SPC/E<sup>10</sup> and TIP4P<sup>11</sup>, are of Lennard-Jones (LJ) type and have three superimposed point charges. These models are widely applied, especially in current biochemical research, since they enable simulations of relatively large molecular systems at reasonable computational cost. Therefore, most force fields for biomolecules, like AMBER<sup>12</sup>, CHARMM<sup>13</sup> and GROMOS<sup>14</sup>, are based on these water models.

For the ions, various force fields have been developed since the 1990s. Early on, ion models often neglected the electrostatic interactions at long distances<sup>15,16</sup> or simple reaction field corrections were used<sup>17</sup>. Peng et al.<sup>18</sup> were the first to analyze different models for alkali and halide ions in aqueous solutions, using the consistent force field<sup>19</sup> for water. The result of their study was a set of molecular ion models that reproduces several solid state properties and the microscopic liquid solution structure with a fair accuracy. With increasing computing power and more advanced simulation techniques, the molecular representations of ion solutions became more reliable and thereby the accuracy of the models increased. Weerasinghe and Smith developed molecular models for sodium chloride<sup>20</sup> and guanidinium chloride<sup>21</sup> in aqueous solution using the Kirkwood-Buff theory<sup>22</sup>. The resulting models show a very good agreement with experimental data for these two solutions, especially for the liquid solution density. The Kirkwood-Buff theory and the activity calculations were recently extended to all alkali chloride combinations<sup>23</sup> and to all alkali halide salts<sup>24</sup>. In another approach, Reif and Hünenberger<sup>25</sup> derived force fields for alkali and halide ions on the basis of the hydration free energy. The result of their parameterization strategy are

six different parameter sets for all alkali cations and halide anions due to the “absence of precise experimental values”<sup>25</sup> for the hydration free energy. The authors point out that trustworthy experimental hydration free energy data are not yet available<sup>25</sup>. Horinek et al.<sup>26</sup> used the free energy and the enthalpy of solvation to optimize force fields of alkali and halide ions. Their study resulted in one unique parameter set for the anions, while for the cations, three parameter sets were proposed that describe the energy of hydration equally well. In a subsequent work of that group, Fyta et al.<sup>27</sup> reoptimized the ion force fields for a subset of the alkali halide salt models. The target properties for the optimization were the solvation free energy and the osmotic coefficient. An improvement of the force fields for potassium and cesium was obtained, but the study did not converge on a parameter set for fluoride and iodide. This problem was solved by Fyta and Netz<sup>28</sup> by introducing cation-anion interaction parameters. Their force fields for  $K^+$ ,  $Cs^+$ ,  $F^-$  and  $I^-$  were parameterized to the single-ion solvation free energy, whereas the cation-anion interaction parameters of the alkali cations and the halide anions were adjusted via Kirkwood-Buff theory. The resulting two parameter sets for potassium, cesium, fluoride and iodide in combination with the corresponding cation-anion interaction parameters yield good results for the solution activity, the excess coordination number and the osmotic coefficient. Wheeler and Newman<sup>29</sup> focused on two distinct brines: sodium chloride and potassium chloride in water. Here, the ion models were parameterized to reproduce both the liquid solution density and the self-diffusion coefficient of the ions in aqueous solution. The resulting parameter set<sup>29</sup> captures the liquid solution density for both saline solutions in good agreement with experimental data. These force fields were assessed with respect to other transport properties of the liquid electrolyte solution like viscosity and electric conductivity.

A recent study by our group<sup>30</sup> led to one unique force field set for the alkali and halide ions in aqueous solution based on the LJ approach with one superimposed point charge of magnitude +1 and -1 e for cation and anion, respectively. Here, the LJ size parameter  $\sigma_i$  was adjusted simultaneously for nine ions to the reduced liquid solution density  $\tilde{\rho}$  of all 19 relevant aqueous solutions of alkali halide salts. The reduced liquid solution density is defined by  $\tilde{\rho} = \rho/\rho_w$ , where  $\rho$  is the liquid density of the solution and  $\rho_w$  the density of pure water, both at the same temperature and pressure. This property is advantageous for ion force field parameterization, since it is dominated by the presence of the ions in solution and hence, the ion-water interactions. The influence of the solvent, namely the water-water interactions, on the reduced liquid solution density is weak, i.e. the ion LJ size parameter is little dependent on the employed solvent model. The ion force fields

were reported to predict the reduced liquid solution density well for five widely used water models<sup>30</sup> that are based on the LJ approach with superimposed point charges, namely SPC<sup>9</sup>, SPC/E<sup>10</sup>, TIP3P<sup>11</sup>, TIP4P<sup>11</sup> and TIP4P-Ew<sup>31</sup>. In the same study, the ion LJ energy parameter  $\varepsilon_i$  was reported to show only a minor influence on  $\tilde{\rho}$  over a large range  $50 \text{ K} < \varepsilon_i/k_B < 1000 \text{ K}$  and was estimated to be  $\varepsilon_i/k_B = 100 \text{ K}$  for all anions and cations<sup>30</sup>. Note that  $50 \text{ K} < \varepsilon_i/k_B < 1000 \text{ K}$  covers the full range of other recently published data for this parameter<sup>20,32</sup>.

In the present work, the influence of the LJ energy parameter on the self-diffusion coefficient of the alkali cations and the halide anions in aqueous solutions as well as on the position of the first maximum of the radial distribution function (RDF) of water around the ions was investigated systematically. Both are important properties of aqueous electrolyte solutions which were investigated in numerous simulation studies in the literature<sup>15–17,33–35</sup>, for example in the simulation of electrolyte solutions in nanochannels<sup>36,37</sup>. Based on the results of this study, a new choice for the LJ energy parameter is proposed, which differs from the previously reported value  $\varepsilon_i/k_B = 100 \text{ K}$ <sup>30</sup>. The resulting ion force fields were assessed with respect to the self-diffusion coefficient of the ions, the position of the first maximum of the RDF of water around the ions, the electric conductivity, the hydration dynamics around the ions and the enthalpy of hydration. The applied parameterization strategy differs from the method introduced by Wheeler and Newman<sup>29</sup>, where the LJ size parameter  $\sigma_i$  was adjusted both to the liquid solution density and the self-diffusion coefficient of the ions in aqueous solution, but no adjustment of the LJ energy parameter  $\varepsilon_i$  was carried out<sup>29</sup>.

In Section II, the employed force fields are discussed in detail, considering the influence of the LJ energy parameter of the ions on the reduced liquid solution density. In Section III, the applied analysis methods are briefly introduced. Section IV presents the new force field energy parameter as well as all simulation results. Section V concludes the work.

## II. FORCE FIELDS

Water and the ions were both described by LJ type models with one (ions) and three (water) superimposed point charges, respectively. The employed force field hence writes as

$$u_{ij} = 4\varepsilon_{ij} \left( \left( \frac{\sigma_{ij}}{r_{ij}} \right)^{12} - \left( \frac{\sigma_{ij}}{r_{ij}} \right)^6 \right) + \sum_{l=1}^{N_{C,i}} \sum_{m=1}^{N_{C,j}} \frac{q_l q_m}{4\pi\epsilon_0 r_{lm}}, \quad (1)$$

where  $u_{ij}$  is the potential energy between the particles  $i$  and  $j$  with a distance  $r_{ij}$  between their LJ sites.  $\sigma_{ij}$  and  $\varepsilon_{ij}$  are the LJ parameters for size and energy, respectively,  $q_l$  and  $q_m$  are the charges of the solute or the solvent particles that are at a distance  $r_{lm}$  and  $\epsilon_0$  is the vacuum permittivity. The indices  $l$  and  $m$  count the point charges, while the total number of charges of particle  $i$  is denoted by  $N_{C,i}$ . Note that Eq. 1 is given in a form that includes all interactions, i.e. solvent-solvent, ion-solvent and ion-ion. Throughout the present work, the Lorentz-Berthelot combining rules<sup>38,39</sup> were applied for the unlike LJ interactions. This choice is discussed below. In contrast, other recent works<sup>24,28</sup> rely on other combining rules.

The rigid, non-polarizable force field SPC/E<sup>10</sup> was used here for water. This model is widely applied in molecular simulations of biomolecules, often in combination with the GROMOS force field<sup>14</sup>. The LJ size parameter  $\sigma_i$  of the ion models was taken from preceding work<sup>30</sup>, where it was adjusted to the reduced liquid solution density  $\tilde{\rho}$  in a global fit to data for all aqueous solutions of alkali halide salts<sup>30</sup>. The reduced density  $\tilde{\rho}$  is defined by the liquid density of the solution divided by the density of pure water, both at the same temperature and pressure. The quality of the absolute liquid density data that are obtained for aqueous alkali halide solutions is primarily determined by the quality of the water model. Using the SPC/E water model, which shows a decent agreement with the experimental density of pure liquid water at ambient conditions<sup>10</sup>, the density of aqueous alkali halide solutions was reproduced in good agreement with experimental work<sup>30</sup>. It is well known that the density of mixtures is dominated by the combining rule for the size parameter  $\sigma$ <sup>40</sup>. Note that the Lorentz combining rule yields good results for the density of aqueous electrolyte solutions<sup>30</sup> and hence no introduction of binary interaction parameters for  $\sigma$  is necessary. In our preceding study<sup>30</sup>, the ion LJ energy parameter  $\varepsilon_i$  showed hardly any influence on  $\tilde{\rho}$  over a wide range of parameter values and was hence simply set to a value of  $\varepsilon_i/k_B = 100$  K<sup>30</sup>. However, an influence of  $\varepsilon_i$  on other solution properties is present. It is worthwhile to discuss this influence and the relation between  $\varepsilon_i$  and the electrostatic interaction of the chosen model on the level of the intermolecular interaction. Therefore, the unlike intermolecular potential energy  $u_{\text{Na-H}_2\text{O}}$  was considered here as a function of distance  $r$  between a sodium cation and a water molecule. For the evaluation of this energy, the water molecule was oriented in an energetically favorable configuration so that its negative partial charge points towards the cation, while the hydrogen atoms were at the largest possible distance from the cation. The potential energy function was determined for three values of the LJ energy parameter of the sodium cation, i.e.  $\varepsilon_{\text{Na}}/k_B = 20, 200$  and  $1000$  K, while all remaining model parameters were adopted from our preceding work<sup>30</sup> and were kept

constant. The results are illustrated in Figure 1. Contraintuitive findings can be seen in the plot: the smallest value for the LJ energy parameter  $\varepsilon_{\text{Na}}/k_{\text{B}} = 20$  K leads to the deepest potential well and the well depth of the potential energy decreases significantly with increasing  $\varepsilon_{\text{Na}}$ . The reason for this behavior of the interaction energy is due to the nature of the LJ potential. The choice of the LJ energy parameter  $\varepsilon_i$  also influences the repulsive contribution of the LJ potential, i.e. the lower  $\varepsilon_i$  is, the softer the repulsive interaction becomes. The softening of the repulsive interaction with decreasing  $\varepsilon_i$ , together with the strong electrostatic attraction that acts at short distances between ion and water molecule, leads to the observed deepening of the potential well with decreasing  $\varepsilon_i$ . Hence, for ions in aqueous solutions, lower values of the ion LJ energy parameter  $\varepsilon_i$  lead to a stronger attraction, not vice versa as usual.

Note that the total unlike interaction energy for larger distances  $r$  is almost independent on the ion LJ energy parameter due to the strong electrostatic interaction contribution between ion and water that dominates  $u_{\text{Na-H}_2\text{O}}$ . This dominance is illustrated in Figure 1, where it can be seen that the LJ potential energy for  $\varepsilon_{\text{Na}}/k_{\text{B}} = 1000$  K is small in comparison to the total interaction energy.

In the present study, the influence of the LJ energy parameter of the ions on their aqueous solutions is investigated systematically and the choice for values of  $\varepsilon_i$  is addressed. Note that data on dispersion, determined by quantum mechanical calculations, were not considered in the study. Simulation results for the self-diffusion coefficient of the alkali cations and the halide anions in aqueous solutions as well as the position of the first maximum of the radial distribution function of water around the ions are compared to experimental data. Based on these results, LJ energy force field parameters for alkali cations and halide anions are proposed that reproduce these reference data well. Note that the simple Lorentz-Berthelot combining rule was used to determine the unlike interactions. Throughout the study, diluted electrolyte solutions were investigated. Hence, the LJ energy parameter of the ion  $i$  contributes to the potential energy of the solution predominantly via the unlike interaction  $\varepsilon_{i-\text{H}_2\text{O}} = \sqrt{\varepsilon_i \varepsilon_{\text{H}_2\text{O}}}$ , i.e. the adjustment that was performed here optimizes the description of the interactions between the ions and the water molecules. No additional binary parameters in the Berthelot combining rule were used.

For all simulations of this study, an extended version of the simulation program *ms2*<sup>41</sup> was employed. Technical details are given in the Appendix.

### III. DYNAMIC, STRUCTURAL AND CALORIC SOLUTION PROPERTIES

Molecular simulations of aqueous alkali halide salt solutions were carried out to determine their thermodynamic properties. The following quantities were assessed: the self-diffusion coefficient  $D_i$  of the ions, the RDF  $g_{i-O}(r)$  of water around the ion  $i$ , the electric conductivity  $\sigma$ , the hydration dynamics around the ions, i.e. residence time  $\tau_{i-O}$  which quantifies the time that a water molecule remains in the first hydration shell around an ion  $i$ , the energy barrier  $\Delta w^{\max}$  for water molecules leaving the first hydration shell and the enthalpy of hydration  $\Delta h_{\text{hyd,S}}$ . Structural properties, like the hydration number and the net charge, were discussed in our preceding work<sup>30</sup>. Activity data were not determined because the commonly used simulation methods, such as gradual insertion<sup>42-45</sup>, yield results with large statistical uncertainties. Throughout the present paper, the solution composition is given in terms of the mole fraction. The mole fraction  $x_S$  of the salt is the overall mole fraction, i.e. for the 1:1 salts studied here, the mole fractions of the anions and cations are  $x_S$  each.

The self-diffusion coefficient of the ions and the electric conductivity of the aqueous solutions were determined via equilibrium molecular dynamics (MD) simulations by means of the Green-Kubo formalism<sup>46</sup>. This formalism offers a direct relationship between transport coefficient and the time integral of the autocorrelation function of the corresponding flux within a fluid. Hence, the Green-Kubo expression for the self-diffusion coefficient  $D_i$  is based on the individual ion velocity autocorrelation function<sup>46</sup>

$$D_i = \frac{1}{3N_i} \int_0^\infty \langle \mathbf{v}_{ik}(t) \cdot \mathbf{v}_{ik}(0) \rangle dt, \quad (2)$$

where  $\mathbf{v}_{ik}(t)$  is the center of mass velocity vector of ion  $k$  of species  $i$  at some time  $t$ . Eq. 2 is an average over all  $N_i$  ions of species  $i$ .

The electric conductivity  $\sigma$  is related to the time autocorrelation function of the electric current flux  $\mathbf{j}(t)$  and is given by<sup>47</sup>

$$\sigma = \frac{1}{3Vk_B T} \int_0^\infty \langle \mathbf{j}(t) \cdot \mathbf{j}(0) \rangle dt, \quad (3)$$

where  $V$  is the volume. The electric current flux is defined by the charge  $q_k$  of ion  $k$  and its velocity vector  $\mathbf{v}_k$  according to

$$\mathbf{j}(t) = \sum_{k=1}^{N_{\text{Ion}}} q_k \cdot \mathbf{v}_k(t), \quad (4)$$

where  $N_{\text{Ion}}$  is the number of ions in solution. Note that for evaluating Eq. 4 all ions have to be considered, but not the water molecules. For better statistics,  $\sigma$  was determined for all three

independent spatial elements of  $\mathbf{j}(t)$ . The electric current time autocorrelation function may be decomposed into the sum<sup>48</sup>

$$\langle \mathbf{j}(t) \cdot \mathbf{j}(0) \rangle = \underbrace{\sum_{k=1}^{N_{\text{Ion}}} \langle q_k^2 \cdot \mathbf{v}_k(t) \cdot \mathbf{v}_k(0) \rangle}_{Z(t)} + \underbrace{\sum_{k=1}^{N_{\text{Ion}}} \sum_{\substack{n=1 \\ n \neq k}}^{N_{\text{Ion}}} \langle q_k q_n \cdot \mathbf{v}_k(t) \cdot \mathbf{v}_n(0) \rangle}_{\Delta(t)}, \quad (5)$$

where  $Z(t)$  is an autocorrelation function and  $\Delta(t)$  is a crosscorrelation function that quantifies the deviations from the ideal Nernst-Einstein behavior<sup>48,49</sup>.

The first term  $Z(t)$  describes the mobility of the ions due to their self-diffusion in solution. Mathematically, it is directly related to the sum of the velocity autocorrelation functions of all ion types in solution weighted by their charges. The second term  $\Delta(t)$  describes the correlated motions of the ions in solution. Correlated motions of ion pairs of opposite charges in solution decrease the electric conductivity ( $\Delta(t) < 0$ ), while correlated motions of ion pairs with the same charges increase it ( $\Delta(t) > 0$ ). The magnitude of the electric conductivity is highly dependent on the salinity, i.e. it increases with  $x_S$ .

The RDF  $g_{i-O}(r)$  of water around the ion  $i$  indicates the microscopic structure that the ion imposes onto the solution. In this case, the water molecule position was assumed to be the position of the oxygen atom. The RDF is well known from the literature<sup>50</sup> and is not formally introduced here.

Hydration dynamics are characterized by the residence time  $\tau_{i-O}$ , which defines the average time span that a water molecule remains within a given distance  $r_{i-O}$  around an ion  $i$ . It is related to the following autocorrelation function<sup>17</sup>

$$\tau_{i-O} = \int_{t=0}^{\infty} \left\langle \frac{1}{n_{i-O}} \sum_{k=1}^{n_{i-O}} \Theta_k(t) \Theta_k(0) \right\rangle dt, \quad (6)$$

where  $t$  is the time,  $n_{i-O}$  is the hydration number around ion  $i$  at  $t = 0$  and  $\Theta$  is the Heavyside step function, which yields unity, if the water molecule is paired with the ion. In this study, the residence time of water in the first hydration shell was determined. A water molecule and an ion were considered as paired, if their distance  $r_{i-O}$  was smaller than the position of the first minimum of the RDF, i.e.  $r_{i-O} < r_{\text{min},1}$ . Following a proposal by Impey et al.<sup>51</sup>, unpairing of an ion and a water molecule was assumed when their separation ( $r_{i-O} > r_{\text{min},1}$ ) lasts more than 2 ps. However, a short-time pairing of two particles  $\tau_{i-O} < 2$  ps was fully accounted for in the calculation  $\tau_{i-O}$ .

The energy barrier  $\Delta w^{\text{max}}$  that a water molecule has to overcome in order to leave the first hydra-

tion shell was determined from the orientationally averaged ion-water RDF by<sup>17,52,53</sup>

$$w_{i-O}(r) = -k_B T \ln g_{i-O}(r) . \quad (7)$$

Here,  $w_{i-O}$  is the potential of mean force between ion  $i$  and the surrounding water molecules. The energy barrier is defined as the difference between the numbers for  $w_{i-O}$  at the first minimum and the first maximum of the potential of mean force.

In addition, the enthalpy of hydration of the salt  $\Delta h_{\text{hyd},S}$  was investigated. It is defined as the difference between the partial molar enthalpy of the salt dissolved in the aqueous solution at infinite dilution and the molar enthalpy of the salt in an artificial ideal gas reference state. Using molecular simulation,  $\Delta h_{\text{hyd},S}$  can be derived from the enthalpy of a highly dilute aqueous electrolyte solution  $H_S$  and the enthalpy of the pure solvent  $H_{\text{H}_2\text{O}}$  divided by the mole number of the salt in the solution  $n_S$ <sup>54</sup>

$$\Delta h_{\text{hyd},S} = \frac{H_S - H_{\text{H}_2\text{O}}}{n_S} - k_B T . \quad (8)$$

The enthalpy of hydration was determined here accordingly for all alkali halide salts individually.

## IV. RESULTS

The self-diffusion coefficient  $D_i$  of the ions in aqueous solution as well as the RDF  $g_{i-O}(r)$  of water around the ion  $i$  were chosen to specify the LJ energy parameter of the ion models. All remaining properties were subsequently determined in a strictly predictive manner.

### A. Model adjustment I - Self-diffusion coefficient

The self-diffusion coefficient of the alkali cations and the halide anions in aqueous solutions was determined for a salt mole fraction of  $x_S = 0.009$  mol/mol. A low salinity reduces the influence of correlated motions between anion and cation so that the values of  $D_i$  are hardly dependent on the counterion in solution. Numerous aqueous alkali halide solutions were investigated so that  $D_i$  of every ion was determined at least for two different counterions. The self-diffusion coefficient of each ion was determined as a function of its LJ energy parameter, which was varied between

$20 \text{ K} \leq \varepsilon_i/k_B \leq 1000 \text{ K}$ . The results for the alkali cations are shown in Figure 2 and for the halide anions in Figure 3.

The influence of the salt concentration on the self-diffusion coefficients of these ions is, in comparison to the values at infinite dilution, weak at this low salinity<sup>33–35</sup>. Nevertheless, experimental self-diffusion coefficients<sup>55</sup> measured at the salt mole fraction matching the simulations were used in this study to exclude additional errors.

### 1. Alkali cations

*Lithium and Sodium:* For the self-diffusion coefficient of  $\text{Li}^+$  and  $\text{Na}^+$ , hardly any dependence on the LJ energy parameter was found.  $D_i$  is practically constant for  $20 \text{ K} \leq \varepsilon_i/k_B \leq 1000 \text{ K}$ . The value of  $D_{\text{Li}}$  from simulation is in excellent agreement with the experimental data<sup>55</sup>.  $D_{\text{Na}}$  from simulation exhibits an offset of about 20 %. The low sensitivity of  $D_{\text{Li}}$  and  $D_{\text{Na}}$  on the LJ energy parameter is due to the strong electrostatic attraction between these ions and the water molecules in the first hydration shell. Lithium and sodium cations do not diffuse as single particles in aqueous solution, but together with their first hydration shell. Their  $D_i$  is thus dominated by the diffusivity of the ion-water complex and therefore, on the molecular level, by the interactions of the water molecules in the first hydration shell around  $\text{Li}^+$  and  $\text{Na}^+$  with the bulk water molecules. Thus,  $\varepsilon_i$  has a negligible influence on  $D_i$ . The strong attraction between these two cations and the water molecules in their first shell can also be seen in the hydration dynamics, where the energy barrier for a water molecule leaving the first shell is very high, cf. Section IV G.

*Potassium, Rubidium and Cesium:* In case of  $\text{K}^+$ ,  $\text{Rb}^+$  and  $\text{Cs}^+$ , the influence of the LJ energy parameter on the self-diffusion coefficient is much more pronounced. For  $\varepsilon_i/k_B < 200 \text{ K}$ , a decrease of  $D_i$  was found. For such low values of  $\varepsilon_i$ , the repulsive interaction between ion and water is weaker (as illustrated in Figure 1) and as a consequence, the ion-water complex becomes more stable, which hinders the ion motion in bulk solution. For a large LJ energy parameter of  $\varepsilon_i/k_B > 700 \text{ K}$ , the self-diffusion coefficient is decreased as well. In case of such high values of  $\varepsilon_i$ , the thermal motions of the ions are more constrained to the first cage of solvent molecules around the ion. A strong repulsion between ion and water hinders the diffusion of the ion in solution, which leads to a lower  $D_i$ . With increasing size of the ions, the attraction between the surrounding water molecules and the charge of the ion is less pronounced and thus the thermal motions of

larger ions are reduced by lower  $\varepsilon_i$ . Hence, a slight decrease of  $D_i$  was observed already for  $\varepsilon_i/k_B = 400$  K in case of the larger rubidium and cesium cations.

For intermediate values of  $200 \text{ K} \leq \varepsilon_K/k_B \leq 400 \text{ K}$ , the self-diffusion coefficient of potassium shows an excellent agreement with experimental data<sup>55</sup>, the deviations are below 5 %. The large range of the LJ energy parameter that reproduces the experimental data well is due to the mutual compensation of the two effects described above. The self-diffusion coefficients of rubidium and cesium ions for  $\varepsilon_i/k_B = 200$  K are also in excellent agreement with the experimental data<sup>55</sup>. The simulation results are within the experimental uncertainty of about 2 %.

## 2. Halide anions

For all halide anions, a similar behavior of the self-diffusion coefficient as for the larger cations ( $\text{K}^+$ ,  $\text{Rb}^+$  and  $\text{Cs}^+$ ) was observed. Again, both for high and low  $\varepsilon_i$  values, a decrease of  $D_i$  was found for the reasons discussed above.

*Fluoride:* In the case of the fluoride ion, the maximum of  $D_F$  was observed for  $\varepsilon_F/k_B = 400$  K. As the peak value of  $D_F$  is above the experimental data, there are two different values for the LJ energy parameter of  $\text{F}^-$  where the deviation from the experimental value is zero, cf. Figure 3. Hence, both  $\varepsilon_F/k_B = 200$  K and  $\varepsilon_F/k_B = 700$  K are acceptable parameters.

*Chloride and Bromide:* The chloride and bromide self-diffusion coefficients are almost constant in the parameter ranges  $200 \text{ K} \leq \varepsilon_{\text{Cl}}/k_B \leq 700 \text{ K}$  and  $200 \text{ K} \leq \varepsilon_{\text{Br}}/k_B \leq 400 \text{ K}$ . The thermal motions of the larger bromide anion are constrained for lower  $\varepsilon_i$  values, since the attraction between the surrounding water molecules is less pronounced in comparison to the  $\text{Cl}^-$  anion. In the corresponding ranges, the deviations between simulation and experiment are below 10 %.

*Iodide:* As for the rubidium and cesium cation, the self-diffusion coefficient of  $\text{I}^-$  has a maximum value at a LJ energy parameter  $\varepsilon_I/k_B = 200$  K. In that case,  $D_I$  is in excellent agreement with the experimental data. The deviations are below 5 %.

## B. Model adjustment II - Radial distribution function

For the choice of reasonable  $\varepsilon_i$  values of all ions, the parameter range derived from the self-diffusion coefficient was further restricted by considering another property, i.e. the position of the first maximum  $r_{\max,1}$  of the RDF  $g_{i-O}(r)$  of water around the alkali cations and the halide anions in aqueous solution. The RDF was determined for a salt mole fraction of  $x_S = 0.01$  mol/mol. At such a low salinity, the occurrence of ion pairing between anions and cations is reduced so that the values of  $r_{\max,1}$  are hardly dependent on the counterion in solution. The RDF of water around the ions were calculated for aqueous LiCl, NaBr, KF, RbI and CsCl solutions. The water molecule position was represented in these simulations by the position of the oxygen atom. The dependence of the first maximum  $r_{\max,1}$  on the LJ energy parameter was studied in the range from  $100 \text{ K} \leq \varepsilon_i/k_B \leq 700 \text{ K}$ . The simulation results and the ranges of experimental  $r_{\max,1}$  values<sup>56,57</sup> for the alkali cations and the halide anions are shown in Figure 4 and Figure 5, respectively.

As expected, the position  $r_{\max,1}$  increases with increasing size of the ion. This can be seen both from the experimental data and the simulation results for the alkali cations and the halide anions. Note that the LJ site of  $\text{Li}^+$  and  $\text{Na}^+$  has nearly the same size ( $\sigma_{\text{Li}} = 1.88 \text{ \AA}$ ,  $\sigma_{\text{Na}} = 1.89 \text{ \AA}$ ) and hence the simulation results for  $r_{\max,1}$  are practically identical for these two cations. As discussed in preceding work<sup>30</sup>, the dependence of  $r_{\max,1}$  on  $\varepsilon_i$  is weak. Nevertheless, a trend is observable, which can be used for the specification of the LJ energy parameter of the ions. With increasing  $\varepsilon_i$ , an increase of  $r_{\max,1}$  was observed for all ions (cf. Figure 4 and Figure 5). This can be attributed to the influence of  $\varepsilon_i$  on the intermolecular potential energy between ion and water, which is illustrated in Figure 1 for  $u_{\text{Na-H}_2\text{O}}$ . With increasing  $\varepsilon_i$ , the position of the well depth of the potential energy increases, which accordingly leads to stronger repulsive forces at larger distances.

### 1. Alkali cations

*Lithium:* The simulation results for  $r_{\max,1}$  are within the range of the experimental data for  $\varepsilon_{\text{Li}}/k_B \leq 200 \text{ K}$ . For  $\varepsilon_{\text{Li}}/k_B > 200 \text{ K}$ , the deviation from the experimental data increases with increasing  $\varepsilon_i$ .

*Sodium:* A comparison between the experimental data and the simulation results for  $r_{\max,1}$  indicates that the LJ size parameter  $\sigma_{\text{Na}}$  of the sodium ion from our preceding work<sup>30</sup> is too small.

The simulation results are below the experimental data for  $100 \text{ K} \leq \varepsilon_{\text{Na}}/k_{\text{B}} \leq 700 \text{ K}$ . The smallest deviation of the simulation results from the experimental data was found for  $\varepsilon_{\text{Na}}/k_{\text{B}} = 700 \text{ K}$  and the deviation increases with decreasing  $\varepsilon_i$ . According to the order of the elements in the periodic table,  $\text{Na}^+$  should have a noticeably larger LJ size parameter than  $\text{Li}^+$ . Because the LJ size parameters were adjusted in a systematic manner to the reduced liquid solution density of all aqueous alkali halide solutions<sup>30</sup>, the LJ size parameter of  $\text{Na}^+$  was not reparameterized here.

*Potassium:* For the potassium cation, the simulation results for  $r_{\text{max},1}$  are within the range of the experimental data in the entire LJ energy parameter range  $100 \text{ K} \leq \varepsilon_{\text{K}}/k_{\text{B}} \leq 700 \text{ K}$ .

*Rubidium:* In case of  $\text{Rb}^+$ , the position of the first maximum is within the range of the experimental data only for  $\varepsilon_{\text{Rb}}/k_{\text{B}} = 200 \text{ K}$ . Both for lower and higher  $\varepsilon_i$ , the deviation from the experimental data increases.

*Cesium:* For  $\text{Cs}^+$ , the simulation results for  $r_{\text{max},1}$  are within the range of the experimental data for  $\varepsilon_{\text{Cs}}/k_{\text{B}} < 400 \text{ K}$ . Like for the lithium and rubidium cation, the deviation from the experimental data increases with increasing  $\varepsilon_i$ .

## 2. Halide anions

*Fluoride and Chloride:* For both  $\text{F}^-$  and  $\text{Cl}^-$ , the simulation results for the first maximum of the RDF are above the experimental data for all investigated  $\varepsilon_i$  values. This indicates that the LJ size parameters of these anions are too large. As discussed in case of the sodium cation, a reparameterization was not made here. The smallest deviations from the experimental data were found for both anions for  $\varepsilon_i/k_{\text{B}} = 100 \text{ K}$  and the deviation further increases with increasing  $\varepsilon_i$ .

*Bromide:* The simulation results for  $r_{\text{max},1}$  are within the range of the experimental data for  $\varepsilon_{\text{Br}}/k_{\text{B}} \leq 100 \text{ K}$ . For values of the LJ energy parameter of  $\varepsilon_{\text{Br}}/k_{\text{B}} > 100 \text{ K}$ , the deviation of the simulation results from the experimental data increases with increasing  $\varepsilon_i$ .

*Iodide:* In case of  $\text{I}^-$ , the simulation results for the first maximum of the RDF are within the range of the experimental data for  $100 \text{ K} < \varepsilon_{\text{I}}/k_{\text{B}} < 400 \text{ K}$ . The deviation from the experimental data increases both for decreasing values of  $\varepsilon_{\text{I}}/k_{\text{B}} < 100 \text{ K}$  and increasing values of  $\varepsilon_{\text{I}}/k_{\text{B}} > 400 \text{ K}$ .

### C. Choice of dispersion parameters

The major target for the adjustment of the LJ energy parameter of the ion force fields was the self-diffusion coefficient of the ions in aqueous solution. The dependence of the position of the first maximum of the RDF of water around the ions on  $\varepsilon_i$  was used to restrict the parameter range derived from the self-diffusion coefficient. The LJ energy parameter of the ion force fields was determined to be the  $\varepsilon_i$  value within the parameter range derived from the self-diffusion coefficient which has the smallest deviation of the simulation results for  $r_{\max,1}$  from the experimental data. In case that for  $\varepsilon_i$  a parameter range remains after the restriction by  $r_{\max,1}$ , the LJ energy parameter was set to a selected value from this parameter range.

*Alkali cations:* Both for  $\text{Li}^+$  and  $\text{K}^+$  ranges for the LJ energy parameters were derived from the model adjustment, i.e.  $100 \text{ K} \leq \varepsilon_{\text{Li}}/k_{\text{B}} \leq 200 \text{ K}$  and  $200 \text{ K} \leq \varepsilon_{\text{K}}/k_{\text{B}} \leq 400 \text{ K}$ , respectively. According to the results for the adjustment of  $\varepsilon_i$  of the other force fields, the LJ energy parameter of the lithium and the potassium cations was also set to  $\varepsilon_i/k_{\text{B}} = 200 \text{ K}$ . Here, an adjustment of  $\varepsilon_{\text{Na}}$  was not feasible. However, to be consistent with the other alkali and halide ion force fields  $\varepsilon_{\text{Na}}/k_{\text{B}} = 200 \text{ K}$  was chosen as well. For  $\text{Rb}^+$  and  $\text{Cs}^+$ , the model adjustment to the self-diffusion coefficient and the first maximum  $r_{\max,1}$  of the RDF  $g_{i-\text{O}}(r)$  of water around the ions yields  $\varepsilon_i/k_{\text{B}} = 200 \text{ K}$ .

*Halide anions:* The adjustment of the LJ energy parameter of the ion force fields of the halide anions, i.e.  $\text{F}^-$ ,  $\text{Cl}^-$ ,  $\text{Br}^-$  and  $\text{I}^-$ , yields for all anions  $\varepsilon_i/k_{\text{B}} = 200 \text{ K}$  as described above .

The present study of the self-diffusion coefficient  $D_i$  and the first maximum  $r_{\max,1}$  of the RDF  $g_{i-\text{O}}(r)$  of water around the ions indicates that  $\varepsilon_i/k_{\text{B}} = 200 \text{ K}$  is a reasonable choice for all alkali cations as well as all halide anions. For the applied parameterization strategy of the ion force fields, i.e. adjustment of the LJ size parameter to the reduced liquid solution density and subsequent adjustment of the LJ energy parameter  $\varepsilon_i$  to  $D_i$  and  $r_{\max,1}$ , this single LJ energy parameter value for all alkali cations and all halide anions represents an adequate choice.

As reported in our previous study<sup>30</sup>, the LJ energy parameter shows only a minor influence on  $\tilde{\rho}$  over the range of  $20 \text{ K} \leq \varepsilon_i/k_{\text{B}} \leq 1000 \text{ K}$ . However, the choice of  $\varepsilon_i/k_{\text{B}} = 200 \text{ K}$  leads to slightly different values for  $\tilde{\rho}$  in comparison to the previous work<sup>30</sup>, which will be discussed in detail in a by Reiser et al.<sup>58</sup>.

#### D. Self-diffusion coefficient

The self-diffusion coefficient  $D_i$  was investigated for all alkali cations and halide anions in aqueous solution for  $\epsilon_i/k_B = 200$  K. These data were calculated, as already mentioned above, at low salinity ( $x_S = 0.009$  mol/mol) so that correlated motions of the ions were avoided and  $D_i$  is independent on the counterion in solution.

The results are shown in Figure 6 and are listed in numerical form in Table II. The overall agreement of the simulation results with the experimental data is excellent. The deviations are below 10 % for all ions, except for the sodium cation, where the deviation is about 20 %. These simulation results also follow the qualitative trends both from the experiment<sup>55</sup> as well as from simulation studies<sup>15-17</sup>, i.e.  $D_i$  increases with cation and anion size, respectively. Moreover, the changes of the absolute  $D_i$  values become smaller for larger ions (e.g.  $D_I - D_{Br} < D_{Cl} - D_F$ ). This ion size dependence is directly linked to the formation of ion-water complexes. For small ions, the complex is very firmly attached to the ion. Hence, the effective complex radius, that typically dominates ion motion, is larger for smaller ions than for larger ions, where the ion-water complex formation is less pronounced.

Comparing the self-diffusion coefficient data of the cesium cation and the fluoride anion, which have almost the same size, it can be seen that cations diffuse more rapidly in aqueous solutions than anions. This is due to the fact that the different orientations of the water molecules around the positively charged cesium ion and the negatively charged fluoride ion lead to stronger attached water molecules in the hydration shell around the fluoride ion, which is discussed in detail in the following section. This can also be quantified in terms of the energy barrier  $\Delta w^{\max}$  that a water molecule needs to overcome in order to leave as well as the residence time of water molecules in the hydration shell  $\tau_{i-O}$ . While for the cesium cation  $\Delta w^{\max} = 1.5 k_B T$  and  $\tau_{Cs-O} = 1.0$  ps, for the fluoride anion  $\Delta w^{\max} = 2.5 k_B T$  and  $\tau_{F-O} = 1.5$  ps, cf. Table II.

#### E. Position of the first maximum of the radial distribution function

The position of the first maximum  $r_{\max,1}$  of the RDF  $g_{i-O}(r)$  of water around the alkali cations and halide anions was determined for  $\epsilon_i/k_B = 200$  K. These data were calculated at low salinity ( $x_S = 0.01$  mol/mol) so that ion pairing between anions and cations was avoided and  $r_{\max,1}$  is

independent on the counterion in solution.

The results are shown in Figure 7 and are listed in numerical form in Table II. In case of the alkali cations, the simulation results are within the range of the experimental data, except for  $\text{Na}^+$  where the deviation from the experimental data is 5 %. For the halide anions, only the simulation result for  $r_{\text{max},1}$  of the RDF of water around the iodide anion is within the range of the experimental data. The deviations of the simulation results for  $r_{\text{max},1}$  from the experimental data around  $\text{F}^-$  are 12 %, around  $\text{Cl}^-$  7 % and around  $\text{Br}^-$  3 %.

The position of the first maximum of the RDF of water around the ions increases with increasing size both of the alkali cations and halide anions. The dependence of the simulation results for  $r_{\text{max},1}$  on the size of the ions is nearly identical for the cations and the anions, cf. Figure 7. Comparing the position of the first maximum of the RDF of water around the fluoride anion, which is slightly larger, and the cesium cation, a decrease of  $r_{\text{max},1}$  was observed. This can be attributed to the different orientation of the water molecules around the oppositely charged ions. In case of the positive cesium ion, the negatively charged oxygen atom of the water molecule points towards the ion and hence the two positive hydrogen atoms face into the opposite direction. Because the equally charged hydrogen atoms of neighboring water molecules lead to a mutual repulsion, the water molecules are not able to form a strongly attached hydration shell around the cesium cation. In comparison to the orientation of the water molecules around the cesium cation, predominantly only one of the two hydrogen atoms of the water molecule points towards the negatively charged fluoride anion<sup>51</sup>. The second hydrogen atom, which is not pointing towards the ion, is attracted by the oxygen atom of a neighboring water molecule. Hence, the water molecules constitute a more firmly attached hydration shell around the fluoride ion which is closer to the ion.

## F. Electric conductivity

The electric conductivity  $\sigma$  was calculated for aqueous NaCl and CsCl solutions for various salt mole fractions of up to 0.018 mol/mol at a temperature of 298.15 K and a pressure of 1 bar. These specific salts were chosen, because sufficient experimental data<sup>49,59</sup> are available.

The electric conductivity  $\sigma$  predicted by molecular simulation is in excellent agreement with the experimental data<sup>49,59</sup>, cf. Figure 8. The deviations are below 10 % for all studied solutions, except for CsCl at low salinity, where the deviations are up to 20 %.

The simulation trajectories were analyzed in more detail by separating the electric current time correlation function into its two contributions according to Eq. 5, i.e. the autocorrelation term  $Z(t)$  and the crosscorrelation term  $\Delta(t)$ . This analysis was performed exemplarily for two aqueous NaCl and CsCl solutions with the same salinity of  $x_S = 0.018$  mol/mol. The results for  $Z(t)$  and  $\Delta(t)$  are shown in Figure 9 and Figure 10.

In the aqueous NaCl solution, the motions of oppositely charged ions are correlated ( $\Delta(t) < 0$ ) only for short times  $< 0.3$  ps, while for longer times they are completely uncorrelated. For long times, the electric conductivity is thus determined by the self-diffusivity of the single ions in solution.

The oscillations of  $Z(t)$  and  $\Delta(t)$  in Figure 9 are due to the permanent vibrations of the sodium cation within its hydration shell. These short time motions result from the thermal fluctuations of the ion, which are constrained by the firmly attached hydration shell. These short range motions are superimposed to the characteristic long time motions of the cation and do not contribute to the overall electric flux<sup>51</sup>.

In the aqueous CsCl solution, significant oscillations of  $Z(t)$  and  $\Delta(t)$  do not occur, cf. Figure 10. Larger cations fluctuate only little within their hydration shell. Correlated motions ( $\Delta(t) < 0$ ) of oppositely charged ions were observed only for short times  $t < 0.5$  ps. For longer times,  $\Delta(t) > 0$ , which indicates correlated motions of ions with the same charge. The strong attractive forces between oppositely charged ions lead to a frequent exchange of the interaction partners in terms of correlated motions. Hence,  $\Delta(t)$  is dominated for longer times by correlated motions of ions with the same charge, which can be attributed to electrostatic repulsion.

Comparing the behavior of the ions, correlated motions between oppositely charged ions ( $\Delta(t) < 0$ ) were observed for both studied aqueous alkali chloride solutions. For NaCl, the absolute value of  $\Delta(t)$  is significantly smaller than for CsCl. Correlated motions of oppositely charged ions highly depend on the ability of the anion to replace water molecules in the hydration shell of the cation and vice versa. For  $\text{Na}^+$ , the strong attraction between cation and water molecules in the hydration shell hinders the continuous exchange of water molecules. The chloride anion is not able to replace water molecules in the  $\text{Na}^+$  hydration shell and therefore correlated motions are unlikely to occur. In contrast, there is more exchange of water molecules around  $\text{Cs}^+$  and thus correlated motions are more pronounced.

## G. Hydration dynamics

Using the present force fields, cf. Table I, the residence time of a water molecule in the first hydration shell around an ion was investigated. Furthermore, the energy barrier that is associated with solvent molecules leaving the shell was determined. Note that these properties were considered to be independent on the type of counterion in solution. This assumption is reasonable at low salinity as studied here.

The results for the hydration dynamics are summarized in Table II. As expected, the residence time  $\tau_{i-O}$  of water molecules in the first hydration shell around an ion  $i$  decreases with increasing ion size. For the smallest cations, i.e. lithium and sodium, the residence time is between 6.0 and 9.0 ps, which indicates the existence of stable ion-water complexes. For larger cations, the residence time decreases to  $\approx 1$  ps, while for the larger anions, it is as low as 0.8 ps.

The energy required to remove a water molecule from the first hydration shell is directly correlated with the hydration dynamics, cf. Table II. High energy barriers were found for small ions, while with increasing ion size the energy barrier is lower. For the sodium cation  $\Delta w^{\max}$  was determined to be  $5.1 k_B T$ , while for large ions like the iodide anion it was found to be only  $1.5 k_B T$ . These results again exhibit the very strong electrostatic attraction between the small ions and water molecules that leads to stable ion-water complexes.

## H. Enthalpy of hydration

The enthalpy of hydration of all alkali halide salts in aqueous solutions was determined by molecular simulation at low salinity ( $x_S = 0.01$  mol/mol) at a temperature of 298.15 K and a pressure of 1 bar, cf. Table III. Considering that this property was not included in the parameter adjustment, the agreement between data from simulation and experiment<sup>60</sup> is acceptable for all salts. The enthalpy of hydration was underestimated by about 10 - 20 %, which is slightly more than the experimental uncertainty of 10 to 15 %<sup>60</sup>. Particularly large deviations were found for salts containing small ions.

## V. CONCLUSIONS

Molecular models for alkali and halide ions were investigated in aqueous solutions with respect to a variety of thermodynamic properties, namely the self-diffusion coefficient of the ions, the RDF of water molecules around the ions, the electric conductivity, the hydration dynamics and the enthalpy of hydration.

The self-diffusion coefficient of the alkali cations and the halide anions in aqueous solutions  $D_i$  and the first maximum  $r_{\max,1}$  of the RDF of water around the ions were used for specifying the LJ energy parameter of the ion models. A reasonable agreement with experimental data for both quantities was achieved with a single value of  $\varepsilon_i/k_B = 200$  K for all anions and all cations. Due to a fairly insensitive self-diffusion coefficient and position of the first maximum of the RDF,  $\varepsilon_i$  was not determined by classical optimization, but by excluding unfavorable parameter ranges. The self-diffusion coefficient as well as the position of the first maximum of the RDF around all alkali and halide ions in aqueous solution, as determined by molecular simulation with  $\varepsilon_i/k_B = 200$  K, is in good overall agreement with the experimental data.

The present ion models were used for predictive simulations considering other salts and other thermodynamic properties. The electric conductivity  $\sigma$  was predicted for aqueous NaCl and CsCl solutions over a wide range of salinity. The simulation results match with the experimental data excellently. Correlated motions of differently charged ions were found only at short times. Correlated motions of ions with the same charge were observed for the aqueous CsCl solution. They are attributed to the short lifetime of correlated motions of oppositely charged ions and the electrostatic repulsion. For  $\text{Na}^+$ , oscillating high-frequency motions of the ion within its hydration shell were observed, which lead to oscillations of both contributions.

The average residence time for water molecules in the first hydration shell of the cations was between 1.0 and 9.0 ps. For the anions, it was in the range from 0.8 to 1.5 ps. The residence time is larger for small ions, as the attractive forces between ion and water molecules are stronger. This trend was confirmed by the potential of mean force that shows a decreasing energy barrier for water molecules leaving the first hydration shell. For  $\text{Li}^+$  and  $\text{Na}^+$ , the energy barrier was determined to be  $5.1 k_B T$ , while for the largest anion ( $\text{I}^-$ ), the barrier was only  $1.5 k_B T$ .

The enthalpy of hydration was predicted for all alkali halide salts. The results show a good agreement with the experimental data, the deviations are between 10 and 20 %.

A consistent force field set with a constant energy parameter for all alkali cations and halide anions

was provided. The model parameters were adjusted to experimental data, which are available with a high accuracy. The ion force fields well reproduce numerous other properties, both of the single ions and of solutions containing different combinations of alkali cations and halide anions.

## APPENDIX: SIMULATION DETAILS

For all simulations of this study, an extended version of the simulation program *ms2*<sup>41</sup> was employed. In *ms2*, thermophysical properties can be determined for rigid molecular models using Monte-Carlo (MC) or molecular dynamics (MD) simulation techniques. For all simulations, the LJ interaction partners are determined for every time step and MC loop, respectively. Interaction energies between molecules and/or ions are determined explicitly for distances smaller than the cut-off distance  $r_c$ . Simulation uncertainties were estimated with the block average method by Flyvbjerg and Petersen<sup>61</sup>.

The caloric properties were determined by MC simulations in the isothermal-isobaric ensemble at  $T = 298.15$  K and  $p = 1$  bar. Electrostatic long range contributions were considered by Ewald summation<sup>62</sup> with a real space convergence parameter  $\kappa = 5.6$ . The real space cut-off distance was equal to the LJ cut-off distance of 15 Å. The ion and solvent particles were initially placed into a cubic lattice in random order. The simulation volume was cubic, the initial size of the cube was determined by the expected density in solution. A physically reasonable configuration was obtained by 5,000 equilibration loops in the  $NVT$  ensemble, followed by 80,000 relaxation loops in the  $NpT$  ensemble. Thermodynamic averages were obtained by sampling 200,000 loops. Each loop consisted of  $N_{\text{NDF}}/3$  steps, where  $N_{\text{NDF}}$  indicates the total number of mechanical degrees of freedom of the system.

For the calculation of dynamic properties of the aqueous electrolyte solutions, MD simulations were carried out. The self-diffusion coefficient of the ions and the electric conductivity of the solution were calculated with the Green-Kubo formalism<sup>46,47</sup>. First, the density of the electrolyte solution was determined by a isothermal-isobaric ( $NpT$ ) simulation at the desired temperature and pressure. Subsequently, the self-diffusion coefficient was calculated in the canonical ( $NVT$ ) ensemble at the temperature and density resulting from the first step. The sampling length of the velocity and the electric current correlation functions was set to 11 ps and the separation between the origins of two autocorrelation functions was 0.2 ps. Within this time span, all correlation

functions decayed to less than  $1/e$  of their normalized value.

For all MD simulations in the  $NpT$  ensemble, a physically reasonable configuration was attained by 10,000 time steps in the  $NVT$  ensemble and 100,000 time steps for relaxation in the  $NpT$  ensemble, followed by a production run over 500,000 time steps. For simulations in the  $NVT$  ensemble, the equilibration was carried out over 100,000 time steps, followed by a production run of 1,200,000 and 2,400,000 time steps for the calculation of the self-diffusion coefficient and the electric conductivity, respectively. Newton's equations of motion were solved with a Gear predictor-corrector scheme of fifth order with a time step of 1.2 fs. Temperature control was achieved via velocity scaling. The MD unit cell with periodic boundary conditions contained 4500 molecules. This relatively large number of molecules was used here to minimize the influence of finite size effects on the simulation results. Using the Green-Kubo formalism<sup>46,47</sup> for the calculation of transport properties of aqueous systems, Guevara et al.<sup>63</sup> showed that the finite site effect saturates with increasing number of molecules. No significant differences were observed above 2048 molecules<sup>63</sup>. For the calculation of the self-diffusion coefficient, the simulation volume contained 4420 water molecules, 40 alkali ions and 40 chloride ions. The electric conductivity was determined for different compositions. Hence, the number of alkali ions in the simulation volume varied from 4 to 80. The electrostatic long-range contributions were considered in the same way as in case of MC simulations. The real space and LJ cut-off distance was set to 25 Å.

The structural properties were also determined by MD simulations. In a first step, the density of the aqueous alkali halide solution with a salt mole fraction  $x_S = 0.01$  mol/mol was determined in the  $NpT$  ensemble at  $T = 293.15$  K and  $p = 1$  bar. The simulation volume with periodic boundary conditions contained 10 cations, 10 anions and 980 water molecules. The system was relaxed over 10,000 time steps in the  $NVT$  and 100,000 time steps in the  $NpT$  ensemble. The density was sampled over a production run of 2,000,000 time steps. The resulting density was used in a following  $NVT$  simulation at the same temperature, pressure and composition of the different alkali halide solutions for the determination of the RDF of water around the ions. In this case, the system was relaxed over 100,000 time steps in the  $NVT$  ensemble, followed by a production run of 1,000,000 time steps. The RDF was sampled within the cut-off distance of 15 Å with 500 bins. Newton's equations of motion were solved according to the MD simulations mentioned above. The electrostatic long-range corrections were considered by Ewald summation<sup>62</sup>.

## **ACKNOWLEDGMENTS**

The authors gratefully acknowledge financial support by the BMBF "01H08013 - Innovative HPC-Methoden und Einsatz für hochskalierbare Molekulare Simulation" and DFG's Reinhart Koselleck Program as well as computational support by the Steinbuch Centre for Computing under the grants LAMO and MOCOS and the High Performance Computing Center Stuttgart (HLRS) under the grant MMHBF2. The present research was conducted under the auspices of the Boltzmann-Zuse Society of Computational Molecular Engineering (BZS).

## LIST OF FIGURES

- 1 Potential energy  $u_{\text{Na-H}_2\text{O}}/(k_{\text{B}}T)$  between a sodium cation and a water molecule as a function of their distance  $r_{\text{Na-H}_2\text{O}}$ . Water was described with the SPC/E model<sup>10</sup> with its oxygen site oriented towards the cation. The LJ size parameter of the sodium model was taken from the literature<sup>30</sup>, while its LJ energy parameter was varied:  $\varepsilon_{\text{Na}}/k_{\text{B}} = 20 \text{ K}$  (—),  $\varepsilon_{\text{Na}} = 200 \text{ K}$  (- - -) and  $\varepsilon_{\text{Na}}/k_{\text{B}} = 1000 \text{ K}$  (- · -). The LJ contribution  $u_{\text{Na-H}_2\text{O}}^{\text{LJ}}/(k_{\text{B}}T)$  to the pair potential is shown exemplarily for  $\varepsilon_{\text{Na}}/k_{\text{B}} = 1000 \text{ K}$  (···). . . . . 25
- 2 Self-diffusion coefficient of lithium, sodium, potassium, rubidium and cesium cations in aqueous solutions ( $x_{\text{S}} = 0.009 \text{ mol/mol}$ ) at  $T = 298.15 \text{ K}$  and  $p = 1 \text{ bar}$ . Present simulation data (●) are compared to experimental data<sup>55</sup> (- - -). . . . . 26
- 3 Self-diffusion coefficient of fluoride, chloride, bromide and iodide anions in aqueous solutions ( $x_{\text{S}} = 0.009 \text{ mol/mol}$ ) at  $T = 298.15 \text{ K}$  and  $p = 1 \text{ bar}$ . Present simulation data (●) are compared to experimental data<sup>55</sup> (- - -). . . . . 27
- 4 Position of the first maximum  $r_{\text{max},1}$  of the RDF  $g_{i-\text{O}}(r)$  of water around the lithium, sodium, potassium, rubidium and cesium ion in aqueous solutions ( $x_{\text{S}} = 0.01 \text{ mol/mol}$ ) at  $T = 293.15 \text{ K}$  and  $p = 1 \text{ bar}$ . Present simulation data (●) are compared to the range of experimental  $r_{\text{max},1}$  data<sup>56,57</sup> (grey). . . . . 28
- 5 Position of the first maximum  $r_{\text{max},1}$  of the RDF  $g_{i-\text{O}}(r)$  of water around the fluoride, chloride, bromide and iodide ion in aqueous solutions ( $x_{\text{S}} = 0.01 \text{ mol/mol}$ ) at  $T = 293.15 \text{ K}$  and  $p = 1 \text{ bar}$ . Present simulation data (●) are compared to the range of experimental  $r_{\text{max},1}$  data<sup>56,57</sup> (grey). . . . . 29
- 6 Self-diffusion coefficient of alkali cations (●) and halide anions (■) in aqueous solutions ( $x_{\text{S}} = 0.009 \text{ mol/mol}$ ) at  $T = 298.15 \text{ K}$  and  $p = 1 \text{ bar}$ . Simulation results (filled symbols) are compared to experimental data<sup>55</sup> (open symbols). . . . . 30
- 7 Position of the first maximum  $r_{\text{max},1}$  of the RDF  $g_{i-\text{O}}(r)$  of water around the alkali cations (●) and halide anions (■) in aqueous solutions ( $x_{\text{S}} = 0.01 \text{ mol/mol}$ ) at  $T = 293.15 \text{ K}$  and  $p = 1 \text{ bar}$ . Present simulation data (filled symbols) are compared to the range of experimental  $r_{\text{max},1}$  data<sup>56,57</sup> (vertical lines). Note that the simulation data points for lithium and sodium are identical within their statistical uncertainties. 30

8	Electric conductivity $\sigma$ of aqueous NaCl (●) and CsCl (▲) solutions as a function of the salt mole fraction at $T = 298.15$ K and $p = 1$ bar. Simulation results (filled symbols) are compared to experimental data <sup>49,59</sup> (open symbols). . . . .	31
9	Electric current time correlation functions of NaCl in aqueous solution ( $x_{\text{NaCl}} = 0.018$ mol/mol) at $T = 298.15$ K and $p = 1$ bar separated into its autocorrelation function $Z(t)$ (- - -) and crosscorrelation function $\Delta(t)$ (—). . . . .	31
10	Electric current time correlation functions of CsCl in aqueous solution ( $x_{\text{CsCl}} = 0.018$ mol/mol) at $T = 298.15$ K and $p = 1$ bar separated into its autocorrelation function $Z(t)$ (- - -) and crosscorrelation function $\Delta(t)$ (—). . . . .	32

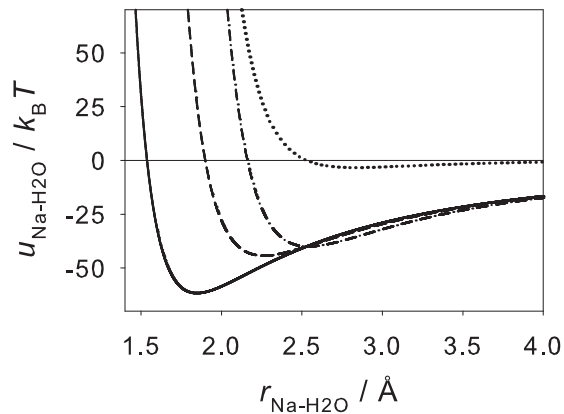


FIG. 1. Potential energy  $u_{\text{Na-H}_2\text{O}}/(k_B T)$  between a sodium cation and a water molecule as a function of their distance  $r_{\text{Na-H}_2\text{O}}$ . Water was described with the SPC/E model<sup>10</sup> with its oxygen site oriented towards the cation. The LJ size parameter of the sodium model was taken from the literature<sup>30</sup>, while its LJ energy parameter was varied:  $\epsilon_{\text{Na}}/k_B = 20$  K (—),  $\epsilon_{\text{Na}} = 200$  K (- - -) and  $\epsilon_{\text{Na}}/k_B = 1000$  K (- · -). The LJ contribution  $u_{\text{Na-H}_2\text{O}}^{\text{LJ}}/(k_B T)$  to the pair potential is shown exemplarily for  $\epsilon_{\text{Na}}/k_B = 1000$  K (···).

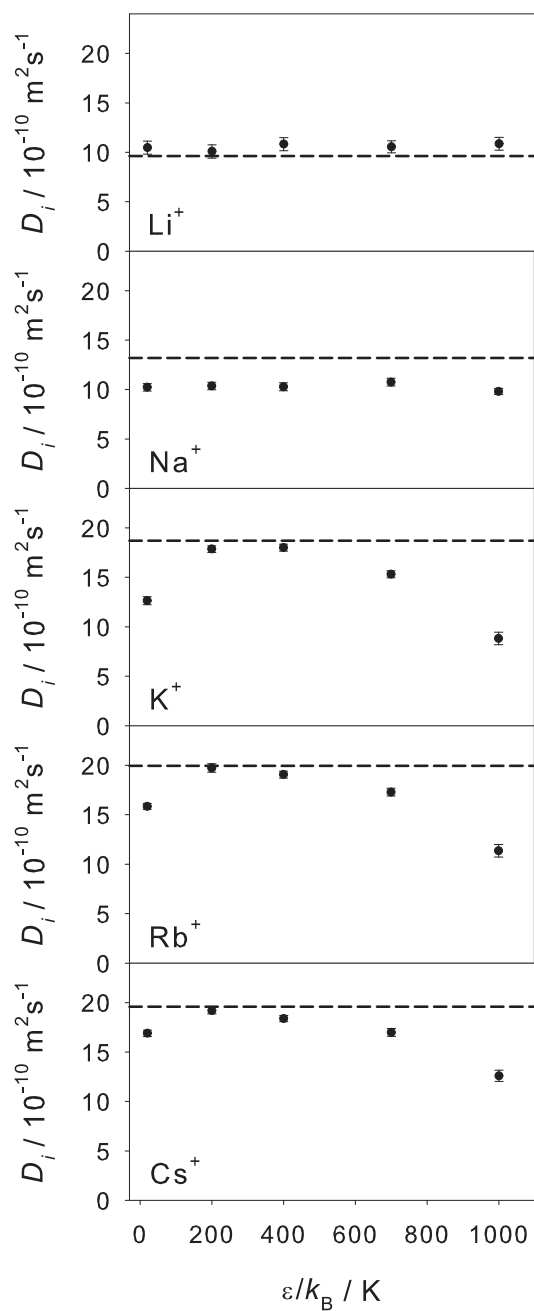


FIG. 2. Self-diffusion coefficient of lithium, sodium, potassium, rubidium, and cesium cations in aqueous solutions ( $x_S = 0.009$  mol/mol) at  $T = 298.15$  K and  $p = 1$  bar. Present simulation data ( $\bullet$ ) are compared to experimental data<sup>55</sup> (- -).

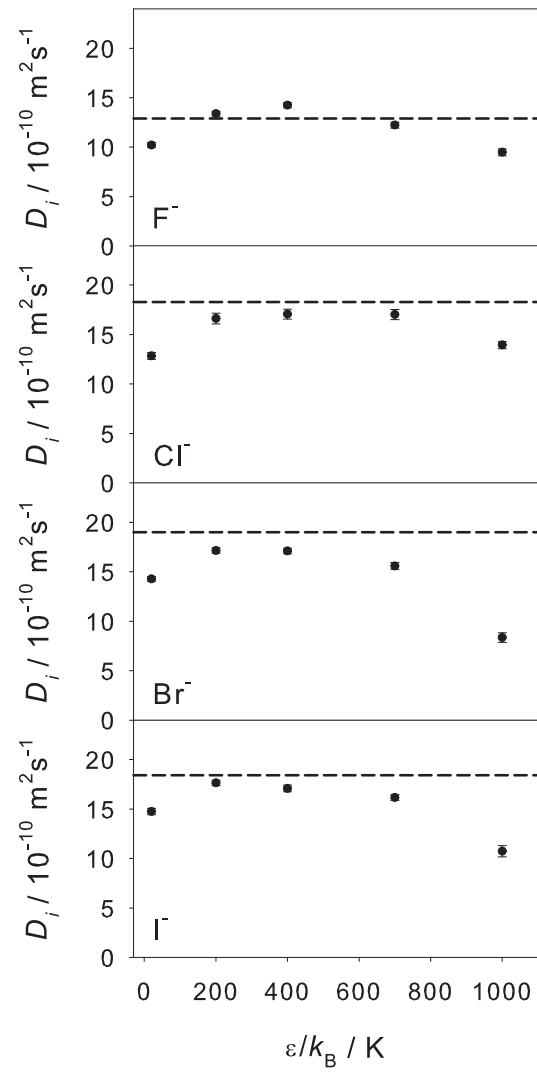


FIG. 3. Self-diffusion coefficient of fluoride, chloride, bromide, and iodide anions in aqueous solutions ( $x_S = 0.009$  mol/mol) at  $T = 298.15$  K and  $p = 1$  bar. Present simulation data ( $\bullet$ ) are compared to experimental data<sup>55</sup> (- -).

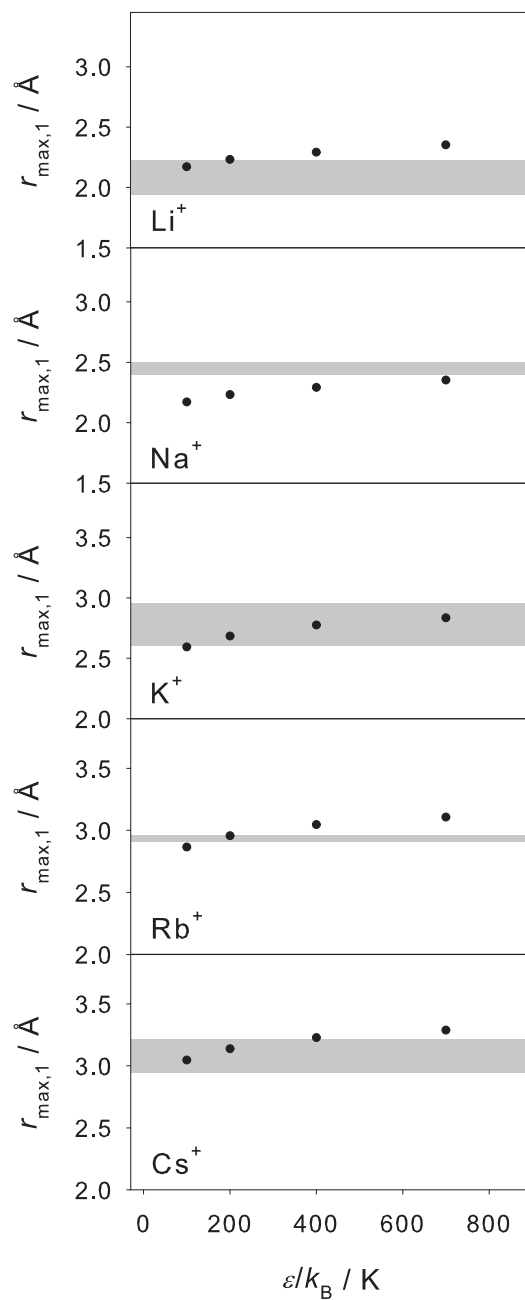


FIG. 4. Position of the first maximum  $r_{\max,1}$  of the RDF  $g_{i-O}(r)$  of water around the lithium, sodium, potassium, rubidium, and cesium ion in aqueous solutions ( $x_S = 0.01$  mol/mol) at  $T = 293.15$  K and  $p = 1$  bar. Present simulation data ( $\bullet$ ) are compared to the range of experimental  $r_{\max,1}$  data<sup>56,57</sup> (grey).

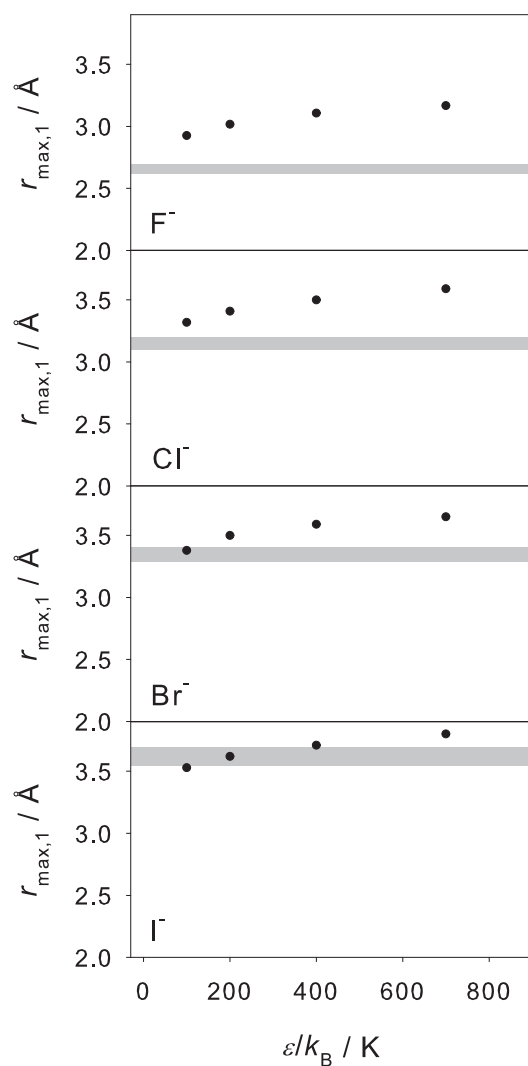


FIG. 5. Position of the first maximum  $r_{\max,1}$  of the RDF  $g_{i-\text{O}}(r)$  of water around the fluoride, chloride, bromide, and iodide ion in aqueous solutions ( $x_S = 0.01$  mol/mol) at  $T = 293.15$  K and  $p = 1$  bar. Present simulation data (●) are compared to the range of experimental  $r_{\max,1}$  data<sup>56,57</sup> (grey).

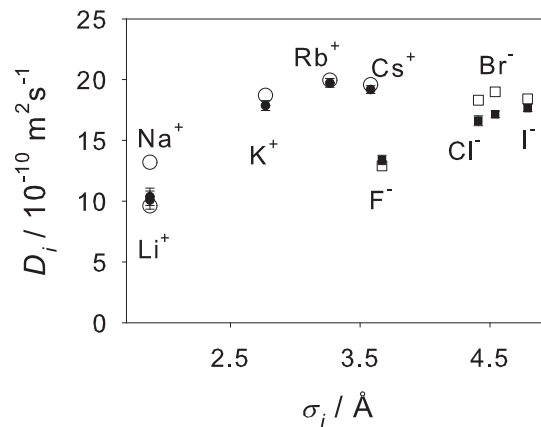


FIG. 6. Self-diffusion coefficient of alkali cations ( $\bullet$ ) and halide anions ( $\blacksquare$ ) in aqueous solutions ( $x_S = 0.009$  mol/mol) at  $T = 298.15$  K and  $p = 1$  bar. Simulation results (filled symbols) are compared to experimental data<sup>55</sup> (open symbols).

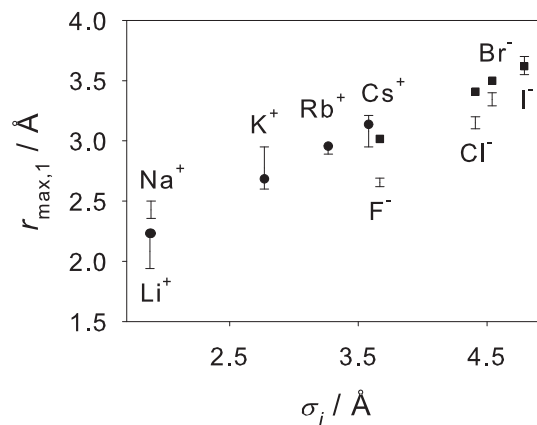


FIG. 7. Position of the first maximum  $r_{\max,1}$  of the RDF  $g_{i-\text{O}}(r)$  of water around the alkali cations ( $\bullet$ ) and halide anions ( $\blacksquare$ ) in aqueous solutions ( $x_S = 0.01$  mol/mol) at  $T = 293.15$  K and  $p = 1$  bar. Present simulation data (filled symbols) are compared to the range of experimental  $r_{\max,1}$  data<sup>56,57</sup> (vertical lines). Note that the simulation data points for lithium and sodium are identical within their statistical uncertainties.

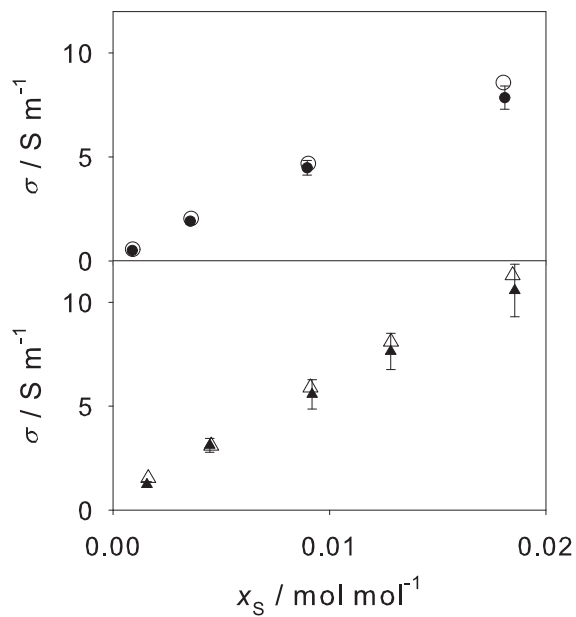


FIG. 8. Electric conductivity  $\sigma$  of aqueous NaCl ( $\bullet$ ) and CsCl ( $\blacktriangle$ ) solutions as a function of the salt mole fraction at  $T = 298.15$  K and  $p = 1$  bar. Simulation results (filled symbols) are compared to experimental data<sup>49,59</sup> (open symbols).

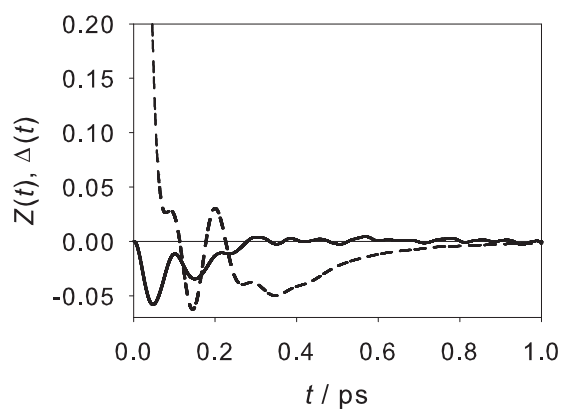


FIG. 9. Electric current time correlation functions of NaCl in aqueous solution ( $x_{\text{NaCl}} = 0.018$  mol/mol) at  $T = 298.15$  K and  $p = 1$  bar separated into its autocorrelation function  $Z(t)$  (---) and crosscorrelation function  $\Delta(t)$  (—).

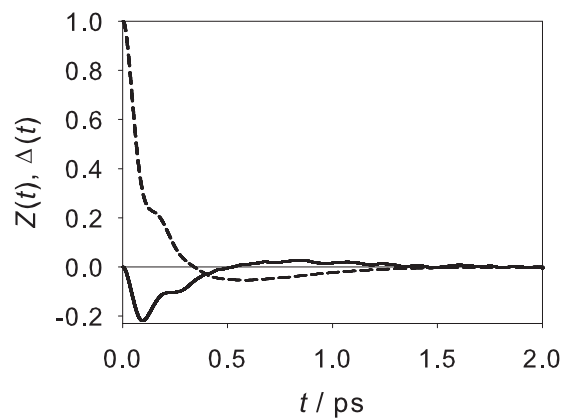


FIG. 10. Electric current time correlation functions of CsCl in aqueous solution ( $x_{\text{CsCl}} = 0.018$  mol/mol) at  $T = 298.15$  K and  $p = 1$  bar separated into its autocorrelation function  $Z(t)$  (- -) and crosscorrelation function  $\Delta(t)$  (—).

TABLE I. LJ size  $\sigma$ , LJ energy  $\varepsilon$  and C6 parameters for dispersion for alkali and halide ions. The size parameters were taken from preceding work<sup>30</sup>.

Ion	$\sigma / \text{\AA}$	$\varepsilon / k_B / \text{K}$	C6 / kcal $\text{\AA}^6 / \text{mol}$	$q / e$
Li <sup>+</sup>	1.88	200	70.19	+1
Na <sup>+</sup>	1.89	200	72.46	+1
K <sup>+</sup>	2.77	200	718.13	+1
Rb <sup>+</sup>	3.26	200	1908.22	+1
Cs <sup>+</sup>	3.58	200	3346.73	+1
F <sup>-</sup>	3.66	200	3821.28	-1
Cl <sup>-</sup>	4.41	200	11693.76	-1
Br <sup>-</sup>	4.54	200	13920.59	-1
I <sup>-</sup>	4.78	200	18962.25	-1

TABLE II. Residence time  $\tau_{i-\text{O}}$  of water in the first hydration shell around ion  $i$ , energy barrier  $\Delta w^{\text{max}}$  for a water molecule leaving the first hydration shell, self-diffusion coefficient  $D_i$  of ion  $i$  and position of the first maximum  $r_{\text{max},1}$  of the RDF  $g_{i-\text{O}}(r)$  of water around the ion  $i$  at  $T = 298.15 \text{ K}$  and  $p = 1 \text{ bar}$ . The number in parentheses indicates the statistical simulation uncertainty in the last digit.

Ion	$\tau_{i-\text{O}} / \text{ps}$	$\Delta w^{\text{max}} / k_B T$	$D_i / 10^{-10} \text{ m}^2 \text{ s}^{-1}$	$r_{\text{max},1} / \text{\AA}$
Li <sup>+</sup>	9.0	5.1	10.1 (7)	2.2
Na <sup>+</sup>	6.0	4.8	10.4 (7)	2.2
K <sup>+</sup>	1.8	2.9	17.9 (4)	2.7
Rb <sup>+</sup>	1.2	1.9	19.7 (4)	3.0
Cs <sup>+</sup>	1.0	1.5	19.2 (3)	3.1
F <sup>-</sup>	1.5	2.5	13.4 (4)	3.0
Cl <sup>-</sup>	1.0	1.7	16.6 (4)	3.4
Br <sup>-</sup>	0.9	1.5	17.2 (3)	3.5
I <sup>-</sup>	0.8	1.3	17.7 (3)	3.6

TABLE III. Enthalpy of hydration  $\Delta h_{\text{hyd},S}$  in kJ/mol for alkali halide salts in aqueous solution at  $T = 298.15 \text{ K}$  and  $p = 1 \text{ bar}$ . The statistical uncertainty was throughout  $\approx 1 \text{ kJ/mol}$ .

Cation	Anion							
	F <sup>-</sup>		Cl <sup>-</sup>		Br <sup>-</sup>		I <sup>-</sup>	
	$\Delta h_{\text{hyd},S}^{\text{Sim.}}$ kJ/mol	$\Delta h_{\text{hyd},S}^{\text{Exp.}}$ kJ/mol						
Li <sup>+</sup>	-831	-1034	-724	-900	-712	-866	-686	-824
Na <sup>+</sup>	-830	-921	-724	-787	-712	-753	-686	-711
K <sup>+</sup>	-711	-837	-606	-703	-594	-669	-567	-627
Rb <sup>+</sup>	-663	-808	-560	-674	-546	-640	-518	-598
Cs <sup>+</sup>	-640	-779	-536	-645	-520	-611	-495	-569

## REFERENCES

- [1] Debye, P.; Hückel, E. *Physikalische Zeitschrift* **1923**, *24*, 185–206.
- [2] Debye, P.; Hückel, E. *Physikalische Zeitschrift* **1923**, *24*, 305–325.
- [3] Chen, C. C.; Britt, H. I.; Boston, J. F.; Evans, L. B. *AIChE Journal* **1982**, *28*, 588–596.
- [4] Chen, C. C.; Evans, L. B. *AIChE Journal* **1986**, *32*, 444–454.
- [5] Pitzer, K. S. *Journal of Physical Chemistry* **1973**, *77*, 268–277.
- [6] Pitzer, K. S.; Mayorga, G. *Journal of Physical Chemistry* **1973**, *77*, 2300–2308.
- [7] Pitzer, K. S.; Mayorga, G. *Journal of Solution Chemistry* **1974**, *3*, 539–546.
- [8] Vega, C.; Abascal, J. L. F. *Physical Chemistry Chemical Physics* **2011**, *13*, 19663–19688.
- [9] Berendsen, H. J. C.; Postma, J. P. M.; van Gunsteren, W. F.; Hermans, J. *Intermolecular Forces*; D. Reidel Publishing Company: Dordrecht, 1981.
- [10] Berendsen, H. J. C.; Grigera, J. R.; Straatsma, T. P. *Journal of Physical Chemistry* **1987**, *91*, 6269–6271.
- [11] Jorgensen, W. L.; Chandrasekhar, J.; Madura, J. D.; Impey, R. W.; Klein, M. L. *The Journal of Chemical Physics* **1983**, *79*, 926–935.
- [12] Ponder, J. W.; Case, D. A. *Protein Simulations* **2003**, *66*, 27–85.
- [13] Brooks, B. R.; Brooks, C. L., III; Mackerell, A. D., Jr.; Nilsson, L.; Petrella, R. J.; Roux, B.; Won, Y.; Archontis, G.; Bartels, C.; Boresch, S.; Caffisch, A.; Caves, L.; Cui, Q.; Dinner, A. R.; Feig, M.; Fischer, S.; Gao, J.; Hodoscek, M. Im, W.; Kuczera, K.; Lazaridis, T.; Ma, J.; Ovchinnikov, V.; Paci, E.; Pastor, R. W.; Post, C. B.; Pu, J. Z.; Schaefer, M.; Tidor, B.; Venable, R. M.; Woodcock, H. L.; Wu, X.; Yang, W.; York, D. M.; Karplus, M. *Journal of Computational Chemistry* **2009**, *30*, 1545–1614.
- [14] Christen, M.; Hünenberger, P. H.; Bakowies, D.; Baron, R.; Burgi, R.; Geerke, D. P.; Heinz, T. N.; Kastenholz, M. A.; Krautler, V.; Oostenbrink, C.; Peter, C.; Trzesniak, D.; van Gunsteren, W. F. *Journal of Computational Chemistry* **2005**, *26*, 1719–1751.
- [15] Lee, S. H.; Rasaiah, J. C. *The Journal of Chemical Physics* **1994**, *101*, 6964–6974.
- [16] Lee, S. H.; Rasaiah, J. C. *Journal of Physical Chemistry* **1996**, *100*, 1420–1425.
- [17] Koneshan, S.; Rasaiah, J. C.; Lynden-Bell, R. M.; Lee, S. H. *Journal of Physical Chemistry B* **1998**, *102*, 4193–4204.
- [18] Peng, Z. W.; Ewig, C. S.; Hwang, M. J.; Waldman, M.; Hagler, A. T. *Journal of Physical Chemistry A* **1997**, *101*, 7243–7252.

- [19]Fabricius, J.; Engelsen, S. B.; Rasmussen, K. *New Journal of Chemistry* **1995**, *19*, 1123–1137.
- [20]Weerasinghe, S.; Smith, P. E. *The Journal of Chemical Physics* **2003**, *119*, 11342–11349.
- [21]Weerasinghe, S.; Smith, P. E. *The Journal of Chemical Physics* **2004**, *121*, 2180–2186.
- [22]Kirkwood, J. G.; Buff, F. P. *The Journal of Chemical Physics* **1951**, *19*, 774–777.
- [23]Klasczyk, B.; Knecht, V. *The Journal of Chemical Physics* **2010**, *132*, 024109.
- [24]Gee, M. B.; Cox, N. R.; Jiao, Y. F.; Bentenitis, N.; Weerasinghe, S.; Smith, P. E. *Journal of Chemical Theory and Computation* **2011**, *7*, 1369–1380.
- [25]Reif, M. M.; Hünenberger, P. H.; *The Journal of Chemical Physics* **2011**, *134*, 144104
- [26]Horinek, D.; Mamatkulov, S. I.; Netz, R. R. *The Journal of Chemical Physics* **2009**, *130*, 124507.
- [27]Fyta, M.; Kalcher, I.; Dzubiella, J.; Vrbka, L.; Netz, R. R. *The Journal of Chemical Physics* **2010**, *132*, 024911.
- [28]Fyta, M.; Netz, R. R.; *The Journal of Chemical Physics* **2012**, *136*, 124103
- [29]Wheeler, D. R.; Newman, J. *Journal of Physical Chemistry B* **2004**, *108*, 18353–18361.
- [30]Deublein, S.; Vrabec, J.; Hasse, H. *The Journal of Chemical Physics* **2012**, *136*, 084501.
- [31]Horn, H. W.; Swope, W. C.; Pitera, J. W.; Madura, J. D.; Dick, T. J.; Hura, G. L.; Head-Gordon, T. *The Journal of Chemical Physics* **2004**, *120*, 9665–9678
- [32]Joung, I. S.; Cheatham, T. E. *Journal of Physical Chemistry B* **2008**, *112*, 9020–9041.
- [33]Koneshan, S.; Rasaiah, J. C. *Journal of Physical Chemistry B* **2000**, *113*, 8125–8137.
- [34]Chowdhuri, S.; Chandra, A. *The Journal of Chemical Physics* **2001**, *115*, 3732–3741.
- [35]Du, H.; Rasaiah, J. C.; Miller, J. D. *Journal of Physical Chemistry B* **2007**, *111*, 209–217.
- [36]Lynden-Bell, R. M.; Rasaiah, J. C. *The Journal of Chemical Physics* **1996**, *105*, 9266–9280.
- [37]Peter, C.; Hummer, G. *Biophysical Journal* **2005**, *89*, 2222–2234.
- [38]Lorentz, H. *Annalen der Physik* **1881**, *248*, 127–136.
- [39]Berthelot, D. *Comptes Rendues de l'Academie des Sciences* **1898**, *126*, 1703–1706.
- [40]Schnabel, T.; Vrabec, J.; Hasse, H. *Journal of Molecular Liquids* **2007**, *135*, 170–178
- [41]Deublein, S.; Eckl, B.; Stoll, J.; Lishchuk, S.; Guevara-Carrion, G.; Glass, C.; Merker, T.; Bernreuther, M.; Hasse, H.; Vrabec, J. *Computer Physics Communications* **2011**, *182*, 2350–2367.
- [42]Lyubartsev, A. P.; Martinovski, A. A.; Shevkunov, S. V.; Vorontsov-Yaminov, P. N. *The Journal of Chemical Physics* **1992**, *96*, 1776–1783.
- [43]Nezbeda, I.; Kolafa, J. *Molecular Simulation* **1991**, *5*, 391–403.

- [44]Lyubartsev, A. P.; Laaksonen, A.; Vorontsov-Velyaminov, P. N. *Molecular Physics* **1994**, *82*, 455–471.
- [45]Vrabec, J.; Hasse, H. *Molecular Physics* **2002**, *100*, 3375–3383.
- [46]Gubbins, K. *Statistical Mechanics Vol. 1*; The Chemical Society Burlington House: London, 1972.
- [47]Hansen, J. P.; McDonald, I. *Theory of Simple Liquids*; Academic Press: Amsterdam, 1986.
- [48]Del Popolo, M. G.; Voth, G. A. *Journal of Physical Chemistry B* **2004**, *108*, 1744–1752.
- [49]Robinson, R. A.; Stokes, R. H. *Electrolyte Solutions*, 2nd ed.; Butterworth: London, 1955.
- [50]Allen, M.; Tildesley, D. *Computer Simulation of Liquids*; Clarendon Press: Oxford, 1987.
- [51]Impey, R. W.; Madden, P. A.; McDonald, I. R. *Journal of Physical Chemistry* **1983**, *87*, 5071–5083.
- [52]Ciccotti, G.; Ferrario, M.; Hynes, J. T.; Kapral, R. *The Journal of Chemical Physics* **1990**, *93*, 7137–7147.
- [53]Rey, R.; Hynes, J. T. *Journal of Physical Chemistry* **1996**, *100*, 5611–5615.
- [54]Chandrasekhar, J.; Jorgensen, W. L. *The Journal of Chemical Physics* **1982**, *77*, 5080–5089.
- [55]Mills, R.; Lobo, V. *Self-diffusion in electrolyte solutions*; Elsevier: New York, 1989.
- [56]Ohtaki, H.; Radnai, T. *Chemical Reviews* **1993**, *93*, 1157–1204.
- [57]Fulton, J. L.; Pfund, D. M.; Wallen, S. L.; Newville, M.; Stern, E. A.; Ma, J. *Journal of Chemical Physics* **1996**, *105*, 2161–2166.
- [58]Reiser, S.; Vrabec, J.; Hasse, H. *in preparation* **2013**.
- [59]Dunsmore, H.; Jalota, S.; Paterson, R. *Journal of the Chemical Society A* **1969**, 1061–1065.
- [60]Riedel, E. *Allgemeine und Anorganische Chemie*, 10th ed.; Gruyter: Berlin, 2010.
- [61]Flyvberg, H.; Petersen, H. *Journal of Chemical Physics* **1989**, *91*, 461.
- [62]Ewald, P. P. *Annalen der Physik* **1921**, *64*, 253–287.
- [63]Guevara-Carrion, G.; Vrabec, J.; Hasse, H. *The Journal of Chemical Physics* **2011**, *134*, 074508.